

Computational Analysis of Free Convection in Different Cavities with Different Aspect Ratios

Manish Bhaskar, Abhinav Saha

Abstract—Cavity and Enclosures are finding increasing applications in the aerospace, marine, transportation, and electrical, chemical, construction and consumer goods industries. In some of these applications the composites are subjected to Thermal loads. This paper deals with the computational analysis of natural convection flow in a square, Cubical, Rectangular, Triangular and trapezoidal cavity, using FEV tool ANSYS FLUENT. Where the bottom wall and vertical walls are heated linearly, and the top wall is been insulated with the maximum temperature T_H and the minimum temperature with T_c . The present numerical investigation deals with steady natural convection flow in a closed square cavity when the bottom wall is sinusoidal heated and vertical walls are linearly heated, whereas the top wall is well insulated. In the nonuniformly heated bottom wall maximum temperature T_H attains at the center of the bottom wall. The sidewalls are linearly heated, maintained at minimum temperature T_c at top edges of the sidewalls and at temperature T_H at the bottom edges of the sidewalls. During convection incompressible fluid is taken and passed over cavities driven by temperature difference across the wall was investigated with different aspect ratio. The temperature distribution and flow pattern across the cavities were visualized. The FEV results are validated with well published results in literature and furthermore with experimentation. Results are first presented in the form of streamlines, isotherm contours, local Nusselt number, and the average Nusselt number as a function of temperature difference aspect ratio.

Index Terms- Natural Convection, Cavity, Nusselt Number.

I. INTRODUCTION

According to [1] natural convection in enclosures in which the initial stage of heating a motionless fluid in a cavity is characterized by an increase in the wall temperature and by a distribution of a temperature wave in the mass of the fluid. Since from 1972, revise of natural convection in field of cavities gave attention toward heating the cavity from bottom walls and side walls. [2] The method accurate solution of the equations describing two-dimensional natural convection in a square cavity with differentially heated side walls computationally was given by [3]. In 1985 semi implicit method in two dimensional flow of viscous incompressible fluid computationally was used.[4] Permanent natural convection in a cavity heated at the base and cooled on the sides was numerically analyzed by [5]. [6] used a numerical approach for night time cooling case, except that the transient simulations were performed and an actual symmetry condition was used at the midplane for Ra up to 7.2×10^4 and $A = 0.2-1.0$.

Manuscript received March, 2014.

Manish Bhaskar, Department of Mechanical Engineering, Shri Shankaracharya College of Engineering and Technology, Junwani, Bhilai, Chhattishgarh, India.

Abhinav Saha, Department of Mechanical Engineering, Shri Shankaracharya College of Engineering and Technology, Junwani, Bhilai, Chhattishgarh, India.

In the case of trapezoidal or triangular cavities, only the natural convection (Rayleigh-Bénard type) was treated. Indeed, a study of natural heat and mass transfer in a trapezoidal cavity heated from below was made by [7]. The results show that for weak slopes, the flow is Rayleigh-Bénard kind. But for high values of the slope, the flow is connected rather with the case of the rectangular cavity type. During 1998 [8] conducted a numerical study in rectangular open cavity. Their results show, for the configuration HB, that heat transfer passes by a maximum for a critical Reynolds number ($Re_m = 100$) corresponding to the disappearance of the cells of recirculation.

In 2002 [9] using control volume method and the SIMPLER algorithm investigated natural convection in isothermal channel with two rectangular ribs, symmetrically located on each wall in laminar flow.

During 2007 steady natural convection flow in a closed square cavity when the bottom wall is sinusoidal heated and vertical walls are linearly heated, whereas the top wall is well insulated is numerical investigated by [10].

Numerical analysis of trapezoidal cavity under mixed convection using a control volume method and the SIMPLER algorithm in order to solve Navier Stokes equation and the effect on Reynolds number under mixed convection is been evaluated by [11].

Numerical simulation of the steady laminar natural convective heat transfer for air within the horizontal annulus between a heated triangular cylinder and its circular cylindrical enclosure and Correlations of the average Nusselt number were proposed based on curve fitting [12].

Unsteady natural convection inside a triangular cavity subject to a non-instantaneous heating on the inclined walls in the form of an imposed temperature which increases linearly up to a prescribed steady value over a prescribed time is reported [13]. The development of the flow from start-up to a steady-state has been described based on scaling analyses and direct numerical simulations. The ramp temperature has been chosen in such a way that the boundary layer is reached a quasi-steady mode before the growth of the temperature is completed. In this mode the thermal boundary layer at first grows in thickness, then contracts with increasing time.

Analysis of natural convection-conduction heat transfer in a square using nanofluids filled in porous medium which is heated by a triangular solid wall was conducted by [14].

Numerical analysis of Natural convection in a two-dimensional porous right-angled triangular enclosure having undulation on the left wall and founded that for small Ra , the heat transfer is dominated by conduction across the fluid layers but with the increase of Ra , the process began to be dominated by convection and the undulation on the left wall play an important role in increasing heat transfer [15].

II. THEORY

The geometry of the problem herein investigated is depicted in Fig. 1.

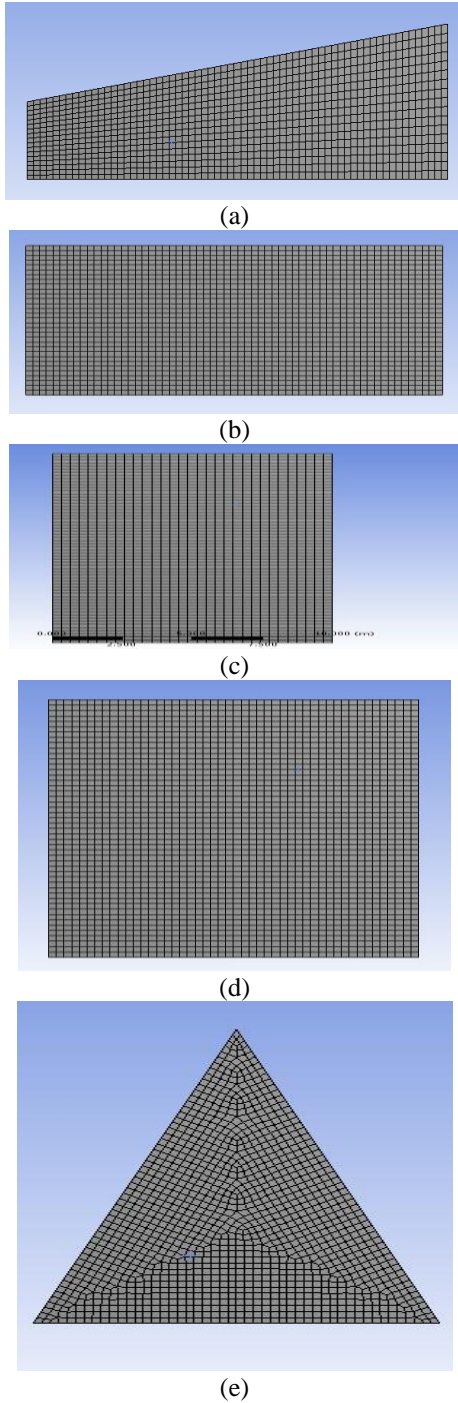


Fig 1 Mesh Configurations.

In system different shapes of cavities are been analyzed with different aspect ratio i.e Rectangular, cubic, Trapezoidal and Triangle. The cavity is heated on its right side and cooled on the opposite side (left), while the top and bottom are maintained isolated. Temperatures of the hot (right) and cold (left) walls are listed as constants, i.e., T_1 and T_0 respectively, while the top and bottom are adiabatic.

The equations governing this problem are those of Navier-Stokes along with the energy equation. The Navier-Stokes equations are applied to incompressible flows and Newtonian fluids, including the continuity equation and the equations of conservation of momentum on the x and y

ACCORDING TO EQUATIONS

$$\frac{\partial u_2}{\partial t} + u_1 \frac{\partial u_1}{\partial x_1} + u_2 \frac{\partial u_1}{\partial x_2} = -\frac{1}{\rho} \frac{\partial p}{\partial x_2} + \nu \left(\frac{\partial^2 u_1}{\partial x_1^2} + \frac{\partial^2 u_1}{\partial x_2^2} \right) + g\beta(T - T_\infty) \quad (1)$$

$$\frac{\partial u_1^*}{\partial x_1^*} + \frac{\partial u_2^*}{\partial x_2^*} = 0 \quad (2)$$

x1 momentum equation

$$\frac{\partial u_1^*}{\partial t^*} + u_1^* \frac{\partial u_1^*}{\partial x_1^*} + u_2^* \frac{\partial u_1^*}{\partial x_2^*} = -\frac{\partial p^*}{\partial x_1^*} + \text{Pr} \left(\frac{\partial^2 u_1^*}{\partial x_1^{*2}} + \frac{\partial^2 u_1^*}{\partial x_2^{*2}} \right) \quad (3)$$

x2 momentum equation

$$\frac{\partial u_2^*}{\partial t^*} + u_1^* \frac{\partial u_2^*}{\partial x_1^*} + u_2^* \frac{\partial u_2^*}{\partial x_2^*} = -\frac{\partial p^*}{\partial x_2^*} + \text{Pr} \left(\frac{\partial^2 u_2^*}{\partial x_1^{*2}} + \frac{\partial^2 u_2^*}{\partial x_2^{*2}} \right) + Gr \text{Pr}^2 T^* \quad (4)$$

Energy equation

$$\frac{\partial T^*}{\partial t^*} + u_1^* \frac{\partial T^*}{\partial x_1^*} + u_2^* \frac{\partial T^*}{\partial x_2^*} = \left(\frac{\partial^2 T^*}{\partial x_1^{*2}} + \frac{\partial^2 T^*}{\partial x_2^{*2}} \right) \quad (5)$$

Where Gr is the Grashof number given as

$$Gr = \frac{g\beta\Delta TL^3}{\nu^2} \quad (6)$$

Often, another non-dimensional number called the Rayleigh number is used in the calculations. This is given as

$$Ra = Gr \text{Pr} = \frac{g\beta\Delta TL^3}{\nu\alpha} \quad (7)$$

Therefore, the effect of Rayleigh number ranging from 105 to 108 was studied for ratios of length to width of the cavity of 0.5, 1, 2 and 3 and the Nusselt number for natural convection.

Triangular

$$\begin{aligned} Gr_H &< 8 \cdot 10^6, T_H > T_o \\ Nu &= C_3 Gr_H^{0.3} \\ Gr_H &= 7 \cdot 10^4 - 5 \cdot 10^5, \\ T_H &< T_o, T_{av} = (T_o + T_H) / 2 \end{aligned} \quad (8)$$

Rec

$$Nu = 0.28 \text{Pr}^{0.024} \left(\frac{H}{B} \right)^{1.75} Ra_H^{0.5}$$

$$H / B = 0.03 - 0.2, \text{Pr} = 1 - 10^3, Ra_H = 10^2 - 10^5$$

$$Nu = 0.851 \text{Pr}^{0.024} \left(\frac{H}{B} \right)^{1.02} Ra_H^{0.25}$$

$$H / B = 0.03 - 0.2, \text{Pr} = 1 - 10^3, Ra_H = 10^5 - 10^6$$

$$Nu = 0.28 \text{Pr}^{0.024} \left(\frac{H}{B} \right)^{0.19} Ra_H^{0.5}$$

$$H / B = 0.2 - 1, \text{Pr} = 1 - 10^3, Ra_H = 10^3 - 10^6 \quad (9)$$

Trapezoidal

$$Nu = C\phi Ra_H^{0.375} \quad (10)$$

$$Ra_H = 10^4 - 10^7 \quad (11)$$

Where $C_\phi = 0.074$ for $\phi = 0^\circ$; $C_\phi = 0.076$ for $\phi = 15 - 30^\circ$; $C_\phi = 0.073$ for $\phi = 45 - 75^\circ$; $C_\phi = 0.07$ for $\phi = 90^\circ$

III. NUMERICAL METHOD

In order to model the problem, the computational modeling and simulation of the numerical is done with the help of ANSYS-FLUENT. In this software platform the numeric simulation of 2D problems involving fluid flow and heat transfer. The program operates for incompressible flow, Newtonian fluid with and without heat transfer, utilizing the Boussinesq approximation in rectangular coordinates (x, y). And with the help of it various temperature profile and isotherms Figures are generated and demonstrated in this paper.

IV. RESULTS

Table I Validation of dimensionless stream function in the case of trapezoidal cavity

	Davis	Quere and Roquefort	Mustapha and Najam	Present (Fluent)
$Ra = 10^4$	5.098	-	5.035	5.032
$Ra = 10^5$	9.667	-	9.725	9.628
$Ra = 10^6$	17.113	16.811	17.152	17.0501
$Ra = 10^7$		30.17		30.152

Table I shows the close and good agreement on comparing results from the present study with those obtained by between the dimensionless stream function in the case of rectangular cavity at various Ra 104 -107. When a steady state is reached, all the energy furnished by the hot wall to the fluid must leave the cavity through the cold surface and the outlet opening. This energy balance is been verified by this references in all cases considered here.

Table II Validation of dimensionless stream function in the case of vertical channel with rectangular blocks.

	Desrayaud and Fichera	Mustapha and Najam	Present (Fluent)
\square_{\max}	151.51	152.85	152.65
M_f	148.27	151.72	151.85

We note that there good agreement was obtained in \square_{\max} and mass flow rate terms in Table II shows the validation of dimensionless stream function in the case of vertical channel with rectangular blocks. The accuracy of the numerical model was verified by comparing results from the present study with those obtained by [9], [11]for natural convection in rectangular block.

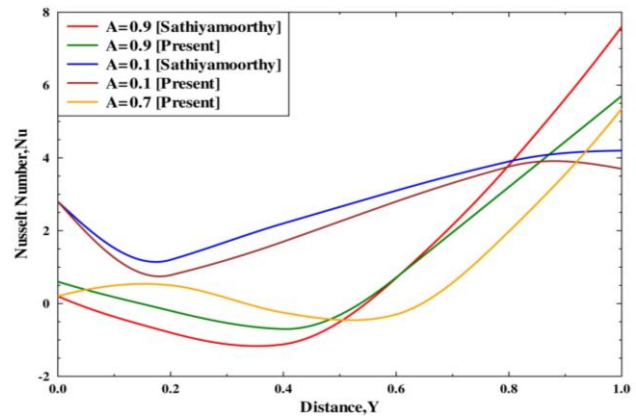


Fig. 2 Variation of local Nusselt number with distance at the side wall in Square cavity for $Pr=0.7$ and $Pr=10$, $Ra=10^5$.

Fig. 2 shows the Variation of local Nusselt number with distance at the side wall in Square cavity for $Pr=0.7$ and $Pr=10$, $Ra=10^5$. from the graph it is illustrated that there is good agreement between the result with the [10] and present one. From this we can revealed that the rate of heat transfer is maximum at the top edge of the side wall because the top wall is insulated as stated in boundary condition. From the Fig. it is concluded that the local heat transfer rate Nu decreases smoothly at the lower half of cavity and simultaneously increases at the upper half of the cavity.

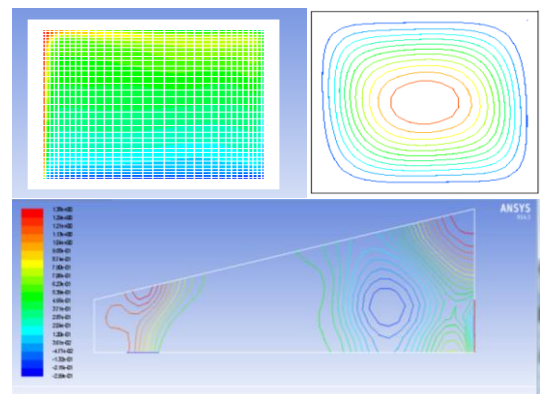
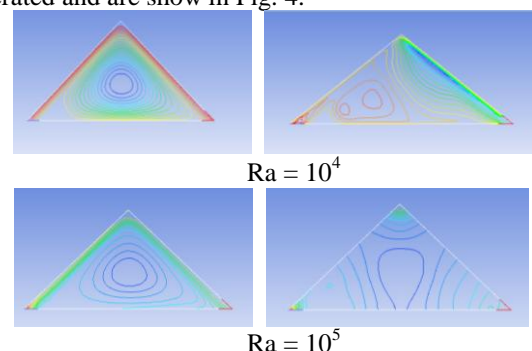


Fig. 3 Temperature profiles and Streamlines inside the Square and Trapezoidal cavity.

Fig. 3 shows the Temperature profiles and Streamlines inside the Square and Trapezoidal cavity which are been generated in FLUENT platform. From this Fig. flow pattern and temperature profile in side cavity can better is examined and heat transfer can better be understood. Similarly for triangular cavity isotherms and temperature profile are generated and are show in Fig. 4.



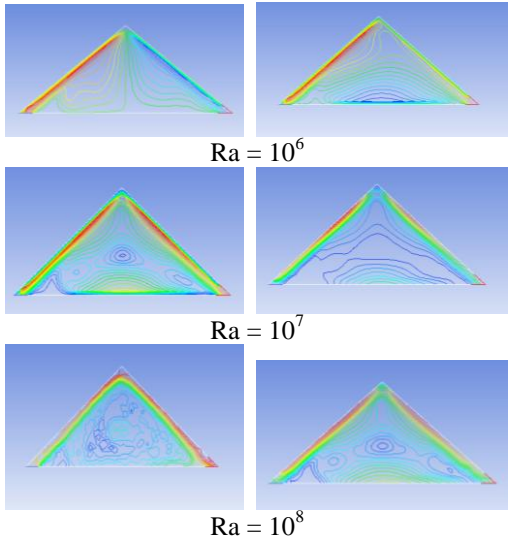


Fig. 4 Temperature profiles and Streamlines inside the Triangular cavities, $Ra\ 10^5$ - 10^8

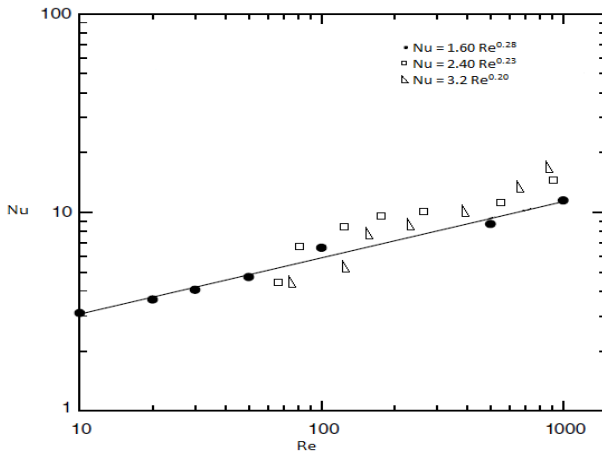


Fig. 5 Nusselt variation with Re for the three studied configurations

The heat transfer through the hot face is given in term of Nusselt number, Fig. 5. It presents the variation of the quantity of a dimensional average heat Q_m according to Re for $Ra = 105$. Generally, Nu increases with Re for the three configurations. This result is awaited because more we increase the speed of the fresh air blast, more we withdraw heat from the cavity towards outside.

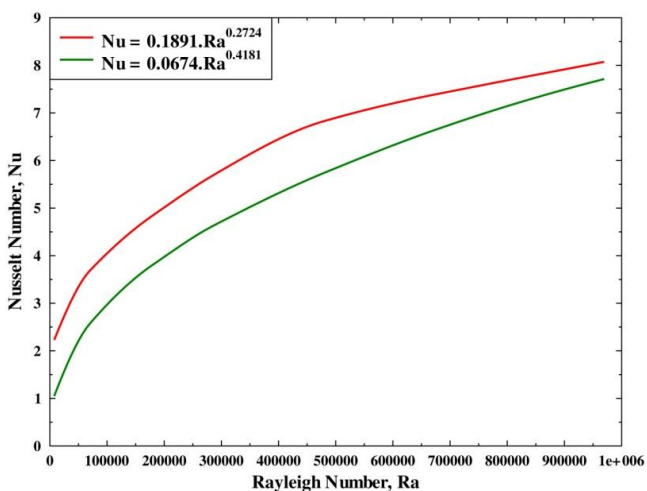


Fig. 6 Correlation between the Nusselt and Rayleigh numbers for $L/D=0.5$ -2.

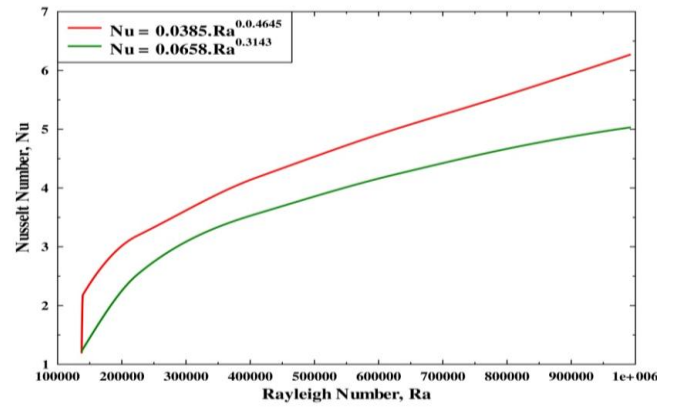


Fig. 7 Correlation between the Nusselt and Rayleigh numbers for $L/D=1$ -3.

From data of the Nusselt number as a function of the Rayleigh number the graphs shown in Figs 6-7 was obtained and the points of the L/D ratio between 0.5 and 3 were plotted. Thus, the equations were obtained that demonstrate the behavior of the Nusselt number as a function of Rayleigh number.

From this it can be concluded that the Total heat transfer through the system depends not only on the Nusselt number in the cavity, as influenced by the Rayleigh number, but also on the thermo physical properties of the wall material and the fluid, and the parameters governing radiation exchange among the cavity walls.

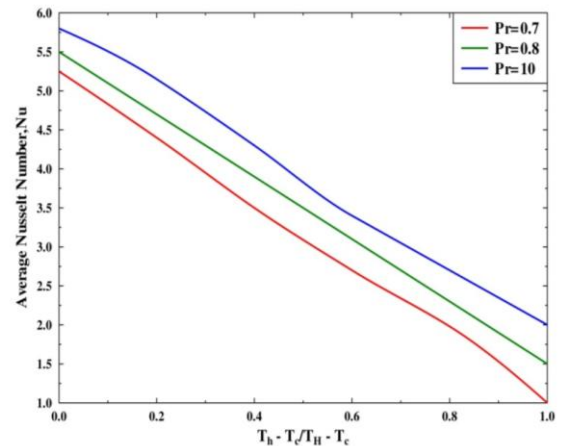


Fig. 8 Variation of average Nusselt number with temperature difference aspect ratio for $Pr=0.7$ and $Pr=10$, at $Ra=10^5$ for bottom wall in square cavity.

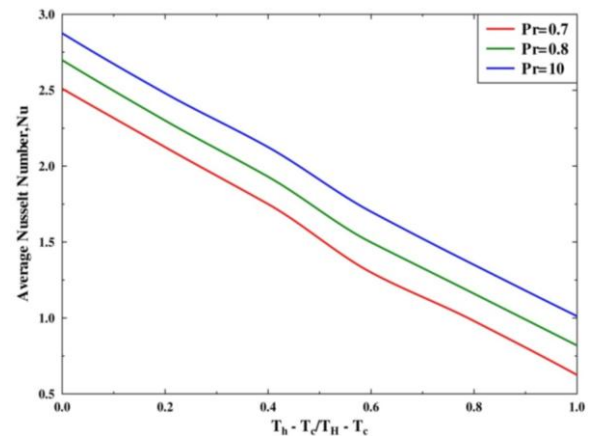


Fig. 9 Variation of average Nusselt number with temperature difference aspect ratio for $Pr=0.7$ and $Pr=10$, at $Ra=10^5$ for Side wall in square cavity

Fig. 8-9 shows the variation of average Nusselt number with temperature difference aspect ratio for $Pr=0.7$ and $Pr=10$, at $Ra=105$ for Side wall in square cavity. It is illustrated from Fig. that, for $Pr=0.7$ and 10, the local Nusselt number Nub decreases locally for all values of $X=0$ and $X=1$ as the temperature aspect ratio increases, from this it can be concluded that the average Nusselt number at the bottom wall linearly decreases as the temperature difference aspect ratio increases for $Pr=0.7$ and 10. Fig. 6.13 shows the boundary conditions at the sidewalls are identical and the top wall is well insulated, the average heat transfer rates follow the relationship $Nus=1/2Nub$, where Nus and Nub are average Nusselt numbers at the sidewall and bottom walls, respectively. Thus, the average Nusselt number at the sidewall also linearly decreases as the temperature aspect ratio increases Fig. 9.

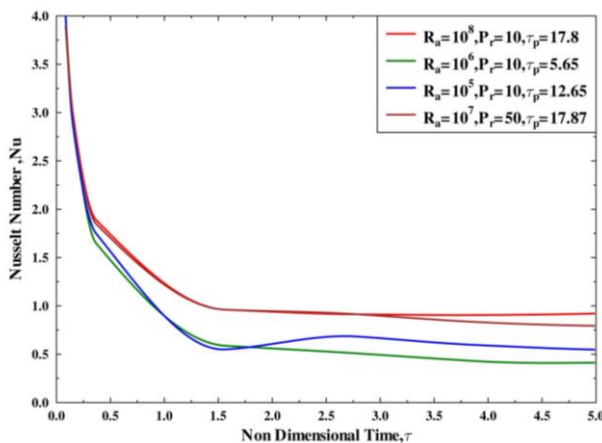


Fig. 10 Nusselt number versus normalized time for 4 runs in triangular cavity.

Fig. 10 shows the Nusselt number variation with time domain of the left inclined wall of the cavity. The Nusselt number is evaluated as same as in previous approach using the instantaneous temperature difference for different Rayleigh numbers, Prandtl numbers and aspect ratios. It is found that the Nusselt number depends strongly on Ra , Pr and A (slope of the inclined wall). Initially the Nusselt number is very high as it is the function of non dimension time. So from the graph it is clear that the all lines collapse together until the ramp is finished which validates the quasi-steady time and Nusselt number scales.

V. CONCLUSIONS

The Rayleigh number significantly influenced the flow profile and heat transfer within the cavity, as well as the thermal boundary layer thickness. It was also found that the Nusselt number strongly depends on the Aspect ratio, and that this dimensionless variable increases with the increasing dimensionless ratio H/B . At the heated vertical wall the Nusselt number increases with a decrease in the wall emissivity e , radiation number N_r , and imposed temperature ratio and increases with the modified Rayleigh number Ra^* , and the Prandtl number Pr . Total heat transfer through the system depends not only on the Nusselt number in the cavity, as influenced by the Rayleigh number, but also on the thermo physical properties of the wall material and the fluid, and the parameters governing radiation exchange among the cavity walls.

REFERENCES

- [1] D. M. Kim and R. Viskanta, "Heat transfer by conduction, natural convection and radiation across a rectangular cellular structure," *International Journal of Heat and Fluid Flow*, vol. 5, No. 4, pp. 205-213, 1984.
- [2] S. Ostrach, "Natural Convection in Enclosures," *Advances in Heat Transfer*, vol. 7, Academic Press, New York, 1972, pp. 161-227.
- [3] G. De Vahl Davis, "Natural convection of air in a square cavity: A bench mark numerical solution," *International Journal for Numerical Methods in Fluids*, vol. 3, issue 3, pp. 249-264, 1983.
- [4] P. Le Queré, T. Alziary de Roquefort "Computation of natural convection in two dimensional cavities with chebyshev polynomials," *Journal of Computational Physics*, vol. 57, Issue 2, pp. 210-228, 1985.
- [5] M. M. Ganzarolli, and L. F. Milanez, "Natural convection in rectangular enclosures heated from below and symmetrically cooled from the sides," *International Journal of Heat and Mass Transfer*, vol. 32, pp. 1063-1073, 1995.
- [6] H. Salmun, "Convection patterns in a triangular domain," *International Journal of Heat and Mass Transfer*, vol. 38, pp. 351-362, 1995.
- [7] M. Boussaid, A. Mezennar, M. Bouhadeb, "Natural convection heat and mass transfer in a trapezoidal cavity (Convection naturelle de chaleur et de masse dans une cavité trapézoïdale)," *Int J Therm Sci.*, vol. 38, pp. 363-371, 1999.
- [8] A. Raji, M. Hasnaoui, "Mixed convection heat transfer in a rectangular cavity ventilated and heated from the side," *Numerical Heat Transfer*, vol. 33, pp. 533-548, 1998.
- [9] G. Desrayaud, A. Fichera, "Laminar natural convection in a vertical isothermal channel with symmetric surface mounted rectangular ribs," *International Journal of Heat and Fluid Flow*, vol. 23, issue 4, pp. 519-529, 2002.
- [10] M. Sathiyamoorthy, T. Basak, S. Roy and N. C. Mahanti, "Effect of the temperature difference aspect ratio on natural convection in a square cavity for nonuniform thermal boundary conditions," *Journal of Heat Transfer*, vol. 129, pp. 1723-1728, 2007.
- [11] I. Tmartnahd, M. El Alami, M. Najam, A. Oubarra, "Numerical investigation on mixed convection flow in a trapezoidal cavity heated from below," *Energy Conversion and Management*, vol. 49, issue 11, pp. 3205-3210, 2008.
- [12] Xu Xu, Gonggang Sun, Yu, Zitao Hu, Yacai Liwu Fan, Kefa Cen, "Numerical investigation of laminar natural convective heat transfer from a horizontal triangular cylinder to its concentric cylindrical enclosure," *International Journal of Heat and Mass Transfer*, Volume 52, Issues 13-14, June 2009, Pages 3176-3186.
- [13] S.C. Saha, "Scaling of free convection heat transfer in a triangular cavity for $Pr > 1$," *Energy and Buildings*, vol. 43, issue 10, pp. 2908-2917, 2011.
- [14] A.J. Chamkha, M.A. Ismael, "Conjugate heat transfer in a porous cavity filled with nanofluids and heated by a triangular thick wall," *International Journal of Thermal Sciences*, vol. 67, pp. 135-151, 2013.
- [15] S. Bhardwaj, A. Dalal, "Analysis of natural convection heat transfer and entropy generation inside porous right-angled triangular enclosure," *International Journal of Heat and Mass Transfer*, vol. 65, pp. 500-513, 2013.

Nomenclature

g	Acceleration due to gravity, $m\ s^{-2}$
k	Thermal conductivity, $W\ m^{-1}\ K^{-1}$
L	Side of the square cavity, m
n	Normal direction on a cavity wall
Nu	Local Nusselt number
P	Dimensionless fluid pressure
Pr	Prandtl number
Ra	Rayleigh number
Re	Reynolds number
Gr	Grashof number
T	Fluid temperature, K
T_c	Temperature of cold top edges of the sidewalls, K

Th	Temperature of hot bottom edges of the sidewall, K
TH	Maximum temperature of middle of the bottom wall, K
A	Aspect ratio of temperature difference, $=T_h - T_c / T_H - T_c$
u	x component of velocity
U	x component of dimensionless velocity
v	y component of velocity
V	y component of dimensionless velocity
X	Dimensionless distance along x coordinate
Y	Dimensionless distance along y coordinate
τ	Non-dimensional time
τ_p	non-dimensional ramp time
ε	Emissivity

Greek Symbols

α	Thermal diffusivity, m^2 / s
β	Thermal expansion coefficient at constant pressure, K^{-1}
ρ	Density, $kg m^{-3}$
c_p	Specific heat coefficient
c_v	Specific heat coefficient
ψ	Stream function
ϕ	Angle

Subscripts

C	cold
H	hot
max	maximum
cr	critical



Manish Bhaskar graduated from Guru Ghasidas University Bilaspur Chhattishgarh India as Mechanical Engg in 2006. His a ME Thermal Eng Scholar at Shri shankaracharya College of Engg & Tech Bhilai CG (Affiliated to Chhattishgara Swami Vivekanand Technical University Bhilai CG India).



Abhinav Saha Completed his Master Of Engg (Thermal engg)from Shri shankaracharya College of Engg & Tech Bhilai CG (Affiliated to Chhattishgara Swami Vivekanand Technical University Bhilai CG India) in 2013.